Bulletin of the Seismological Society of America, Vol. 102, No. 2, pp. 680–695, April 2012, doi: 10.1785/0120110084

Ⓔ

Predominant-Period Site Classification for Response Spectra Prediction Equations in Italy

by Carola Di Alessandro,* Luis Fabian Bonilla, David M. Boore, Antonio Rovelli, and Oona Scotti

Abstract We propose a site-classification scheme based on the predominant period of the site, as determined from the average horizontal-to-vertical (H/V) spectral ratios of ground motion. Our scheme extends Zhao *et al.* (2006) classifications by adding two classes, the most important of which is defined by flat H/V ratios with amplitudes less than 2. The proposed classification is investigated by using 5%-damped response spectra from Italian earthquake records. We select a dataset of 602 three-component analog and digital recordings from 120 earthquakes recorded at 214 seismic stations within a hypocentral distance of 200 km. Selected events are in the moment-magnitude range $4.0 \leq M_w \leq 6.8$ and focal depths from a few kilometers to 46 km. We computed H/V ratios for these data and used them to classify each site into one of six classes. We then investigate the impact of this classification scheme on empirical ground-motion prediction equations (GMPEs) by comparing its performance with that of the conventional rock/soil classification. Although the adopted approach results in only a small reduction of the overall standard deviation, the use of H/V spectral ratios in site classification does capture the signature of sites with flat frequency-response, as well as deep and shallow-soil profiles, characterized by long- and short-period resonance, respectively; in addition, the classification scheme is relatively quick and inexpensive, which is an advantage over schemes based on measurements of shear-wave velocity.

Online Material: Tables of parameters defining the ground motion prediction equations, and figures of H/V spectral ratios, intraevent residuals, and spectral amplitudes.

Introduction

Ground-motion prediction equations (GMPEs) are a fundamental tool in seismic hazard assessment. For the same magnitude and distance, however, variations due to site conditions can be very large and must be properly taken into account in deriving coefficients of the GMPEs. Many recent GMPEs use the value of shear-wave velocity in the uppermost 30 m (V_{S30}) to assign sites to a few classes. Table 1 gives the definitions of two commonly used sets of classes from the American classes (Building Seismic Safety Council, 2000) and the European classes of Eurocode 8 (European Committee for Standardization (CEN), 2004). These velocity-based classifications do have some problems, not the least of which is the limited availability of near-surface shear-wave models at strong-motion sites in many countries. In addition, the cost of obtaining the information can be quite high, especially if based on borehole measurements. A more affordable alternative is velocity profiles inferred from dispersion curves, but they are strictly applicable to 1D situations (see Xia *et al.*, 2002; Di Giulio *et al.*, 2006; Boore and Asten, 2008; Sandıkkaya *et al.*, 2010). Even if V_{S30} values are available, however, the site classes based on these values do not capture the role of the thickness of soft sediments (Steidl, 2000), nor do they capture site resonances in narrow-period bands. The limitation of V_{S30} classes is particularly relevant in deep basins where predictions based on V_{S30} may overestimate ground-motion amplitudes at short periods and underestimate long periods (Park and Hashash, 2004). Including the depth of the uppermost resonant layer in site classification has been recently proposed by Rodríguez-Marek *et al.* (2001) and Pitilakis *et al.* (2006). Cadet *et al.* (2010) investigate whether combining V_{S30} and the fundamental resonance frequency (f_0) is a better way of characterizing sites than using V_{S30} alone. The fundamental frequency of

*Now at: Pacific Earthquake Engineering Research Center (PEER) 325 Davis Hall, University of California–Berkeley, Berkeley, California 94720-1792.

Table 1
Classification Criteria Based on V_{S30} and Soil Properties*

Class	Average Shear-Wave Velocity (V_{S30}) (m/s)	
	NEHRP	EUROCODE 8
A	> 1500	> 800
B	760–1500	360–800
C	360–760	180–360
D	180–360	< 180
E	< 180	Surface alluvium layer with V_S values of type C or D and thickness between 5 and 20 m, underlain by stiffer material with V_S > 800 m/s

*Comparison between the European Seismic Code classes of Eurocode 8 (European Committee for Standardization [CEN], 2004) and the NEHRP scheme (Building Seismic Safety Council, 2000).

the resonant layer has been used as well by Luzi *et al.* (2011) to propose a site classification for Italian stations.

An alternative to V_{S30}-based classes was proposed by Zhao *et al.* (2006), based only on the site predominant period inferred from H/V spectral ratios. This criterion is used in Japan for the seismic design of highway bridges (Japan Road Association, 1980 and its 1990 revision).

Fukushima *et al.* (2007) applied Zhao's classification scheme to a database composed primarily of European earthquakes with a partial contribution of near-source Californian and Japanese earthquakes; the stations that provided the data had originally been classified as rock or soil. While Fukushima *et al.* (2007) were able to unambiguously classify 64% of the total stations, they expressed some concerns on whether there were enough stations that represented the classes that amplify intermediate periods. More recently, a study performed by Ghasemi *et al.* (2009) tested the feasibility of Zhao's classification scheme on Iranian strong-motion stations, attempting three different automatic classification methods but maintaining the same period-range subdivision among the various site classes.

In this paper, we adopt the site-classification method used by Zhao *et al.* (2006) and Fukushima *et al.* (2007) with a few changes. The main difference is the introduction of a new class characterized by flat H/V spectral ratios with amplitudes less than 2. This new class helps in the recognition of reference rock sites. We apply our site classification to the strong-motion stations of the Italian Accelerometric Network (Rete Accelerometrica Nazionale, [RAN]), managed by the Italian Department of Civil Protection (Dipartimento Protezione Civile [DPC]). In addition to assigning a predominant-period class to each recording site, we also classify each site as rock or soil, based on available geotechnical and geological information. The available information for the station characterization presents different refinement levels: it varies from measurements of V_S at 102 sites (45 using cross-hole or down-hole invasive measurements and 57 using noninvasive methods) in the best cases (Di Capua *et al.*, 2011), to subjective characterization based on geological considerations in the worst cases. Our study is part of a research project, sponsored by the DPC (see Acknowledgments) to investigate alternatives to the conventional V_{S30} criteria, with the goal of providing a more homogeneous description of geotechnical and geophysical features at each station to be included as metadata in the strong-motion database of the Italian Accelerometric Archive (ITACA; see Data and Resources).

In this paper we first present the proposed site-classification scheme and use the scheme to classify many sites in Italy that recorded earthquake motions. We then evaluate the new model by applying regression analysis in order to derive GMPEs and to study the interevent and intraevent residuals as well as the standard deviations. Comparison

Table 2
Comparison among the Class Definition Criteria Adopted for the Predominant-Period Classifications in Zhao *et al.* (2006), Fukushima *et al.* (2007), and This Study*

Zhao *et al.* (2006)		Fukushima *et al.* (2007)		Our Proposal	
Site	Description	Site	Description	Site	Description
SC-I	Tg < 0.2 s	SC-1	Tg < 0.2 s	CL-I	Tg < 0.2 s
SC-II	0.2 s ≤ Tg < 0.4 s	SC-2	0.2 s ≤ Tg < 0.6 s	CL-II	0.2 s ≤ Tg < 0.4 s
SC-III	0.4 s ≤ Tg < 0.6 s	SC-3	0.6 s ≤ Tg	CL-III	0.4 s ≤ Tg < 0.6 s
SC-IV	0.6 s ≤ Tg	SC-4	Tg not identifiable and original rock site	CL-IV	0.6 s ≤ Tg
–	–	SC-5	Tg not identifiable and original soil site	CL-V	Tg not idenfiable (flat H/V and amplitude < 2)
–	–	–	–	CL-VI	Broad amplification/ multiple peaks @ Tg < 0.2 s
–	–	–	–	CL-VII	Tg not identifiable (multiple peaks over entire period range)

*Tg is the site natural period (in seconds) as inferred from the H/V spectral ratios.

with predicted spectra based both on the predominant period and commonly used classification criteria in which site classes are based on general geology (e.g., rock or soil) or on V_{S30} are also shown. Finally, we discuss to what extent recorded data from the 6 April 2009 L'Aquila earthquake are matched by our proposed GMPEs (these recordings were not included in the original dataset used to derive our GMPEs and are used only for verification purposes); we find that the site class variations for the L'Aquila earthquake are consistent with those predicted from our GMPEs. This suggests that the site-classification scheme is stable and useful.

Proposed Site Classification

Zhao *et al.* (2006) and Fukushima *et al.* (2007) proposed a classification criterion based on the predominant period of each station identified through the average H/V spectral ratio of the 5%-damped response spectra. In this paper, we apply a similar classification criterion to the Italian dataset.

Our predominant-period classification scheme consists of seven classes. The first four classes (CL-I to CL-IV) are the same as those defined by Zhao *et al.* (2006; Table 2). We further introduce three classes to account for stations that could not be classified as a function of a unique peak in H/V. Independently of the originally available site-category description in terms of geological setting and/or geophysical parameters, we classify a station as generic rock (CL-V) if it displays an almost flat average H/V response spectral ratio with no clear peak and a small overall H/V ratio (<2), whereas we classify it as generic soft soil (CL-VI) if there is a broad amplification at periods longer than 0.2 s or if there is more than one peak and all peaks occur at periods longer than 0.2 s. If multiple peaks are present both before

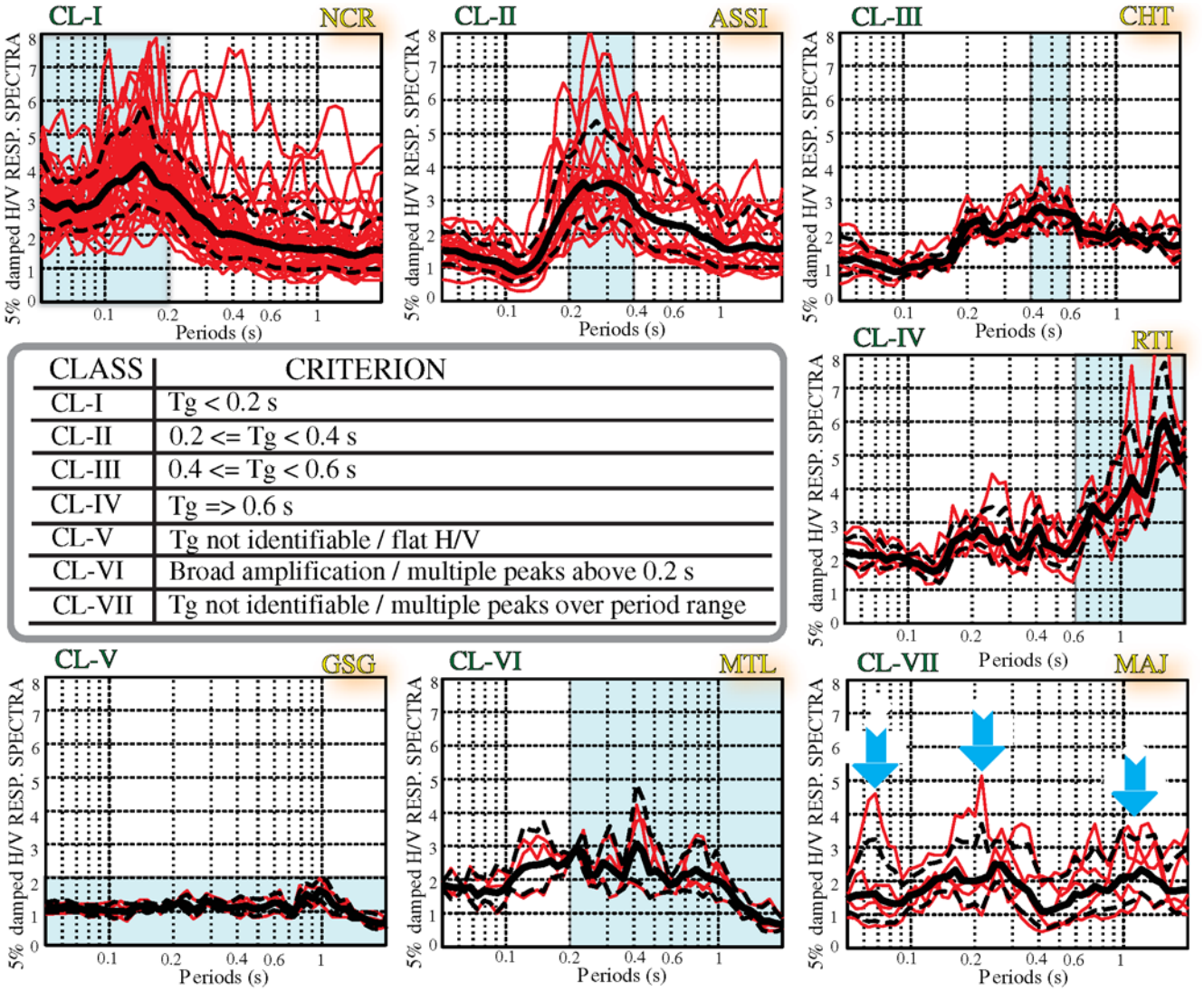

Figure 1. Proposed classification criterion based on the predominant period identified from the average H/V spectral ratio (thick solid line) of the 5%-damped response spectra recorded at each site (thin curves). An example is provided for accelerometer station sites (whose name is displayed at the upper right corner of each panel) that fall into the various classes. The shaded area indicates the interval of validity in which each class is defined. The color version of this figure is available only in the electronic edition.

and after the 0.2-s period threshold, the station cannot be unambiguously classified and therefore it is referred to as unclassifiable (CL-VII). Figure 1 shows examples of stations that were classified according to our proposed classification scheme.

In addition to the classifications based on the predominant period, we also used the geologic information to place each site into one of two classes based on the European classification of Eurocode 8 (European Committee for Standardization [CEN], 2004), where we have lumped A and B and C and D classes together: AB and CD ($V_{S30} \geq 360$ m/s and $V_{S30} < 360$ m/s, respectively (see Table 3). The few sites of class E, as defined in Eurocode 8 (European Committee for Standardization [CEN], 2004), were included in the AB category. In this way, each site has been classified on the basis of its predominant period and of its resemblance to rock (AB) or soil (CD).

Data Used

We study the proposed site classes by using the available digital and digitized analog accelerograms of Italian earthquakes from 1972 to 2004 collected in ITACA strong-motion database (Luzi *et al.*, 2008; Pacor *et al.*, 2011). Additional accelerometric signals for selected recent (2005–2008) events with $M_w > 4.0$ were also included. We supplemented the accelerograms with a small percentage (4%) of broadband velocity-sensor seismograms (converted to acceleration time series via differentiation for the computation of response spectra). The addition of ground motions derived from broadband seismograms helps to better constrain ground motions at distances larger than 100 km, where some GMPEs (e.g., Sabetta and Pugliese, 1996; Bindi *et al.*, 2010) in use for the Italian territory are not applicable, because of the small number of accelerograms available at those distances before the April 2009 L'Aquila earthquake.

After the removal of some stations that were suspected of having soil-structure interaction (S4 project-Deliverable D8, 2009), the time series and Fourier spectra were carefully inspected to make sure that the strongest part of the motions was well recorded and that the signal/noise ratio was greater than a factor of 3 in the frequency range 0.5 to 20 Hz. The final dataset consists of 602 three-component digital and analog recordings from 120 earthquakes recorded at 214 seismic stations within hypocentral distances of 200 km. The moment magnitudes (M_w) range from 4.0 to 6.8. The largest events have focal depths in the range of 5 to 32 km; only one earthquake was deeper (46 km), and it was included in the analysis because its spectral ordinates were consistent in shape and amplitude with those from the shallower earthquakes. Some of the smaller events were at depths less than a few kilometers. The distribution of the records versus magnitude and hypocentral distance is shown in Figure 2.

Table 3
Simplified Classification Adopted in This Paper*

Combined Soil Classes	Average Shear-Wave Velocity (V_{S30})	EUROCODE 8 Classes	NEHRP Classes
AB	$V_{S30} \geq 360$ m/s	A, B, and E	B + C
CD	$V_{S30} < 360$ m/s	C and D	D + E

*Correspondence of the simplified combined soil classification AB and CD with the standard classifications based on V_{S30} for European Seismic Code classes (European Committee for Standardization [CEN], 2004) and NEHRP scheme (Building Seismic Safety Council, 2000).

About 50% of the dataset are from the Friuli, Irpinia, Umbria–Marche, and Molise earthquakes, whose mainshocks had M_w magnitudes of 6.4 (Pondrelli *et al.* 2001), 6.8 (Cocco and Rovelli, 1989), 6.0 (Ekström *et al.*, 1998), and 5.7 (Chiarabba *et al.*, 2005), respectively.

All signals were preprocessed to remove the pre-event mean from the whole record (the zeroth-order correction as defined in Boore *et al.*, 2002; the whole-record mean was used if no pre-event portion was available). A Butterworth fourth-order acausal high-pass filter was then applied to signals after cosine tapering and zero-padding both at the beginning and the end (Boore, 2005; Boore and Bommer, 2005). The length of the zero-padding depends on the order of the filter and on the cutoff frequency according to Converse and Brady (1992). We did not apply low-pass filtering because the Italian accelerometric stations used in this study do not have low kappa values (Rovelli *et al.*, 1988), and therefore response spectra at periods around 0.05 s should not be controlled by higher frequency ground motions (Douglas and Boore, 2011; Akkar *et al.*, 2011).

In order to maintain a consistent filtered dataset and to reduce the influence of the filter cutoff on the usable frequency range, we chose to use response spectra for periods less than 2 s. This choice is consistent with the recommendations by Akkar and Bommer (2006) on the factors that control the useful period range of processed recordings. In

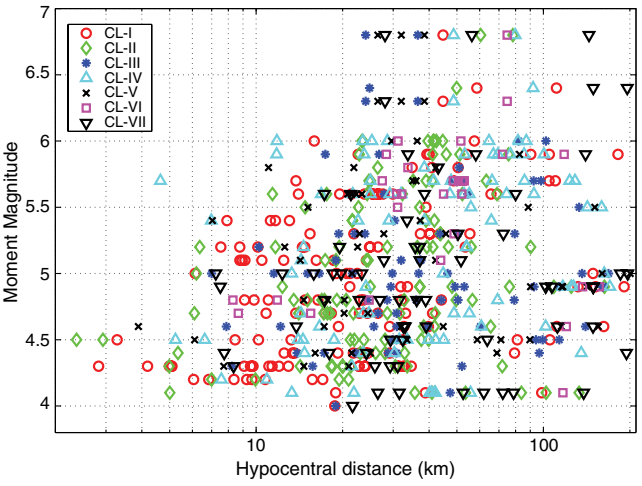

Figure 2. Distribution of moment magnitude and hypocentral distance for the selected dataset. Different symbols correspond to the predominant-period classification scheme proposed in this study. The color version of this figure is available only in the electronic edition.

particular, 2 s corresponds to the 70% of the minimum cutoff period used in the filters (Abrahamson and Silva, 1997; Spudich *et al.*, 1999). Although Paolucci *et al.* (2008) demonstrated that digital accelerograms provide reliable response spectra up to longer periods, the choice of a 2-s upper limit is conservative and conditioned by the use of many analog records (including analog records is necessary if the largest magnitude events in Italy are included in our dataset, as these events were only recorded on analog instruments).

Results of Classifying Italian Strong-Motion Stations

We assigned a classification based on the predominant period for all 214 selected stations. We used the complete dataset for the regression computation, but we considered a subset of 111 stations that recorded more than one event for statistical purposes (see Tables 4, 5, and Fig. 3a,b). The determination of the predominant period of each station was made after computing the average H/V spectral ratio over the events recorded at the station (or over the two horizontal components treated as independent in the case of stations that only recorded a single event). We used ratios of response spectra rather than Fourier spectra (as in Yamazaki and Ansary, 1997), because they do not need subjectively chosen smoothing. The dominant period was determined using the identification procedure proposed by Zhao *et al.* (2004), based on a quadratic function fit to the H/V spectral ratios at three samples around the peak. At the end of this process, we visually inspected the results, and we manually classified some stations for which Zhao's identification procedure gave ambiguous results.

The statistics of the classifications are summarized in Tables 4 and 5, which show cross-tabulation of the stations into the two sets of site classes. Most rock-like AB sites correspond to the new categories CL-I and CL-II, although some are in the more soil-like classes CL-IV and CL-VI. Similarly, soil-like CD sites fall into all but the CL-V classes, with the CL-IV class being the most common. Note that we were able to classify 79 sites out of 91 AB sites and 18 sites out of 20 CD sites using the predominant-period criterion (87% in total, Table 4). The percentage of successful classifications in terms of numbers of records is similar (89%, Table 5).

We computed the geometric mean H/V response spectral ratio and its standard deviation for each site class (Fig. 3a,b). The shape of the mean H/V response spectral ratios are comparable to the results obtained by Zhao *et al.* (2006) for data from Japanese stations (see their fig. 3a,b), at least for the common classes: the periods of the peaks in the mean spectral ratios are consistent with what they found, that is around 0.15 s, 0.25 s, 0.4 s, and 1.0 s for CL-I, CL-II, CL-III, and CL-IV sites, respectively (of course, given that entries in each class are based on the predominant period, it is no surprise that the peaks of the mean ratios are consistent with the site class definitions). As expected on the basis of the class definitions, class CL-V exhibits an almost flat mean H/V response spectral ratio, as we expect for generic rock sites, while class CL-VI displays a broader mean H/V response spectral ratio shape without predominant peaks. The standard deviations have reasonably small values, ranging from 0.2 in natural logarithm scale for class CL-V up to about 0.4 for all the other classes but CL-IV (Fig. 3b). The standard deviation for the latter class is about 0.7 at 0.9-s period. The analysis of the skewness reveals that this high standard deviation value is due to few sites characterized by very high H/V spectral ratios, up to 16, for stations located in basins such as the Aterno Valley and the Po and Garigliano Plains, both characterized by hundreds of meters of alluvial sediments (see De Luca *et al.*, 2005, and Malagnini *et al.*, 1993, respectively). Apart from class CL-IV, in the remaining classes there is a substantial reduction of our standard deviations (20%–40%) compared with the results by Zhao *et al.* (2006) and Fukushima *et al.* (2007), both of whom used a larger dataset. For the sake of example, in the class that amplifies at short periods, our study finds standard deviation below 0.4 in natural logarithm scale, whereas both Zhao *et al.* (2006) and Fukushima *et al.* (2007) find peak values around 0.5. A similar behavior is noted for the class that amplifies at

Table 4
Cross-Tabulation of Stations into the Two Sets of Site Classes

	Number of Stations							
Site Class	CL-I	CL-II	CL-III	CL-IV	CL-V	CL-VI	CL-VII	TOT
AB	19	19	16	11	11	3	12	91
CD	3	2	2	9	0	2	2	20
Total	22	21	18	20	11	5	14	111

Table 5
Cross-Tabulation of Records into the Two Sets of Site Classes

	Number of Records							
Site Class	CL-I	CL-II	CL-III	CL-IV	CL-V	CL-VI	CL-VII	TOT
AB	142	90	72	45	73	12	58	492
CD	13	23	7	46	0	14	7	110
Total	155	113	79	91	73	36	65	602

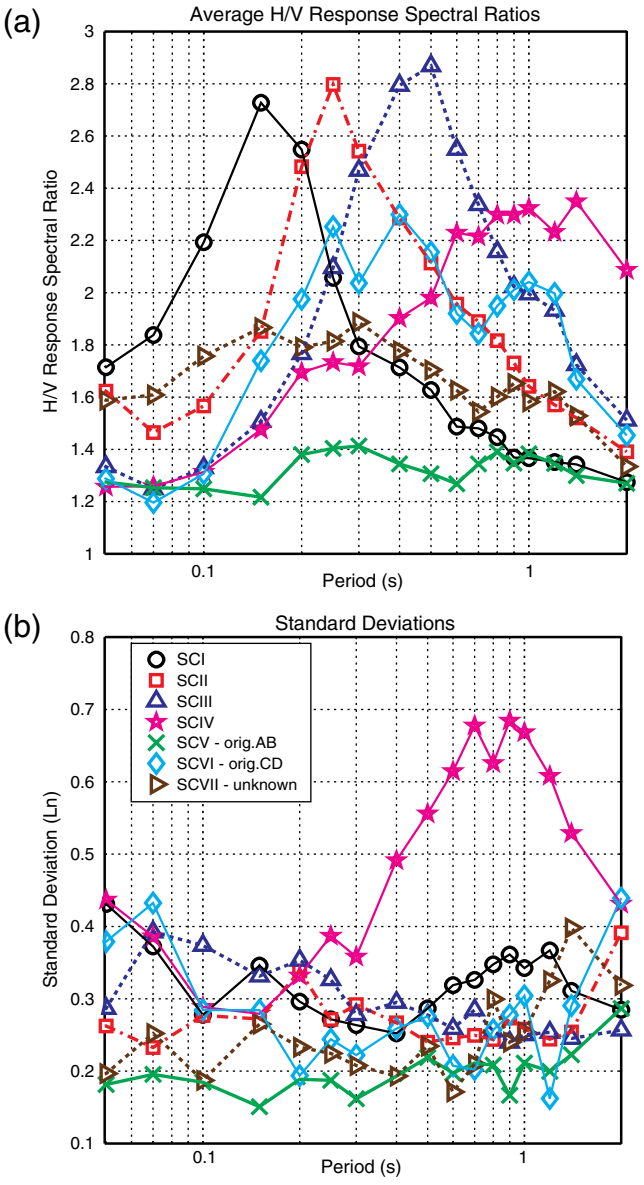

Figure 3. (a) Geometric mean H/V response spectral ratio for each site class proposed in this study, and (b) standard deviations in natural logarithm units. The color version of this figure is available only in the electronic edition.

intermediate periods, where our study finds values below 0.35, whereas both Zhao and Fukushima finds values on the order of 0.5–0.6.

The variations of the H/V spectral ratios between different magnitude and distance ranges are generally not significant. (Ⓔ More results are given in Figs. S1 and S2, and in Tables S2 and S3, available in the electronic supplement to this paper.)

Application of the Proposed Site Classifications

Our evaluation of the proposed site classifications is based on ground-motion prediction equations fit to the data, both with the new site classes and with the simplified rock/soil classification. Figure 2 shows a scatterplot for the distribution of data from different predominant-period classes with respect to moment magnitude and hypocentral distance. A subjective analysis of this figure indicates a relatively uniform distribution of data with respect to moment magnitude and hypocentral distance, where no significant trends can be recognized. This assertion is not based on formal statistical tests, but we feel comfortable asserting that each site class is well represented in the database for a wide range of magnitudes and distances; therefore there should be no bias in deriving the coefficients for the magnitude and distance dependencies in our GMPE. We adopted a similar functional form proposed by Fukushima *et al.* (2007), that is

$$\log_{10} Sa(T) = a(T) + b(T)M + c(T)M^2 + d(T)R - \log_{10}\{R + e(T)10^{fM}\} + S_j(T)\delta_j, \quad (1)$$

where $Sa(T)$ is the elastic absolute response spectral acceleration for 5% damping. The functional form in equation (1) includes magnitude saturation at close distances and a quadratic magnitude dependence of the motions at a fixed distance. $Sa(T)$ was computed from the 602 selected records as the geometric mean of the two horizontal components. In equation (1), a, b, c, d, e, and S_j are period-dependent regression coefficients. f is a period-independent regression coefficient, and M and R are moment magnitude and hypocentral distance (in kilometers), respectively. The suffix j corresponds either to the AB and CD classes or to the seven site classes proposed in this study based on the predominant period. A summation of all site classes, except for AB or CL-I classes, which are taken to be the reference conditions for the site response terms $S_j(T)$, is assumed in the term $S_j(T)\delta_j$, and δ_j is a dummy variable, which is equal to 1 if data are observed at j-th site category and 0 otherwise.

Fukushima *et al.* (2003) used a selection procedure in their dataset in order to exclude small magnitude events at larger distances. We checked this effect in our dataset and realized that such winnowing does not make a strong difference in terms of overall results and standard deviation. Therefore, in order to keep as much data as possible, we did not apply any winnowing as a function of distance and magnitude.

Details of the coefficient computation and comparison with other existing predictive equations at regional and global scale using different site-classification criteria are discussed in the Appendix. The appendix shows a satisfactory agreement with predictions of other regressions that used much larger datasets; we want to stress, however, that the main goal of this study is not the publication of a new GMPE with a limited regional applicability but a check of our new classification scheme comparing its prediction performance with a conventional classification when the same data and same statistics are used. (Ⓔ Coefficients of equation (1) are available in the electronic supplement to this paper.)

Relative amplifications were computed for our classes with respect to a reference class, which was assumed to be the CL-V site class or the AB site class; these amplifications are shown in Figure 4a (although CL-I was chosen as the reference condition in doing the regression, the amplifications can be presented relative to any class; in Fig. 4a we have chosen to use site class CL-V as the reference condition). As shown in that figure, classes CL-I, CL-III, and CL-IV show a comparable amplification factor with respect to CL-V of about 2.5 around 0.13 s, 0.35 s, and above 1 s, respectively, whereas class CL-II shows a lower amplification (1.8 at 0.25 s). This amplification level is similar to the one attained by class CL-VI, even though the latter maintains a broad amplification up to longer periods. Figure 4a also shows interesting high-frequency amplification for site class CL-I. Figure 4a also shows that the relative amplification of CD class with respect to AB resembles closely the one for CL-IV with respect to CL-V, both in terms of spectral shape and amplitude. The fact that both amplifications peak at longer periods is not surprising, but the similarity of the two curves may be a coincidence.

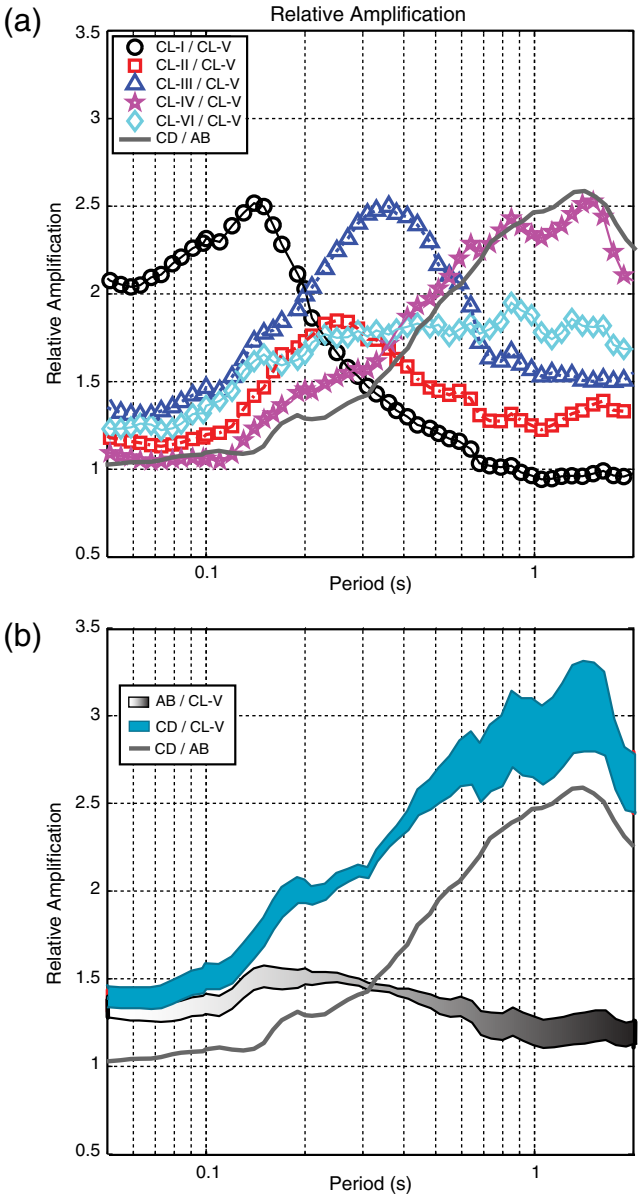

Figure 4. (a) Relative amplification of predominant-period site classes with respect to class CL-V, as well as of CD with respect to AB. (b) Mean ± 1 standard deviation of the relative amplification of AB and CD sites with respect to CL-V as obtained from averaging different scenarios compatible with our dataset. Relative amplification of CD versus in AB is also shown for comparison. The color version of this figure is available only in the electronic edition.

Figure 4b shows relative amplifications between the two types of classes. To compute the predicted relative amplifications for simplified site classes AB and CD with respect to CL-V, we needed to take into account the different magnitude and distance dependencies in the GMPEs for the two ways of classifying sites; therefore, we created a matrix of magnitude-distance couples compatible with our dataset, computed the motions for AB, CD, and CL-V sites, formed the ratios of motions for each magnitude and distance pair, and averaged the ratios over all pairs of magnitude and distance (this procedure was not necessary for Fig. 4a because the magnitude and distance dependency for the predominant-period classes is the same). Figure 4b shows the average ± 1 standard deviation for the predicted relative amplification between AB and CD site classes when CL-V is used as a reference class. Because the AB class includes hard/stiff and shallow soft sites mixed together, Figure 4b shows that, when CL-V is used as the reference, the AB class is amplified up to a factor of 1.5 with a broad shape, and this indicates that the rock class CL-V better captures the main feature of a rock/stiff behavior. Furthermore, relative amplification of the CD class with respect to CL-V has a comparable shape to the one for CD with respect to AB (repeated from Fig. 4a to better allow comparison) but displays higher amplitudes.

Figure 5 shows the effect of our proposed predominant-period classification on corresponding predicted response spectra, compared with the trend shown by our regression using the simplified AB and CD classification and by the GMPEs of Zhao *et al.* (2006) and Fukushima *et al.* (2007) (these were used because they employ a similar site-classification criterion, based on the predominant period). For the sake of example, we plot spectral ordinates for moment magnitudes M_w 4.5 and 6.0 (panels from the bottom to the top) at a hypocentral distance of 50 km. For each magnitude, response spectra for each site class are grouped in terms of the predominant period used to define the site class (amplification at short, intermediate, and long periods, for the left, middle, and right columns of graphs, respectively). Considering only our GMPEs, with respect to the original AB site class the predicted response spectrum for CL-V class shows lower values, especially at short periods (up to 1 s). Conversely, the predicted response spectrum for class CL-I displays higher values. It is worth noticing that the predicted response spectrum for class CL-I has the highest peak value. This effect can be due to weathering of rock or to the presence

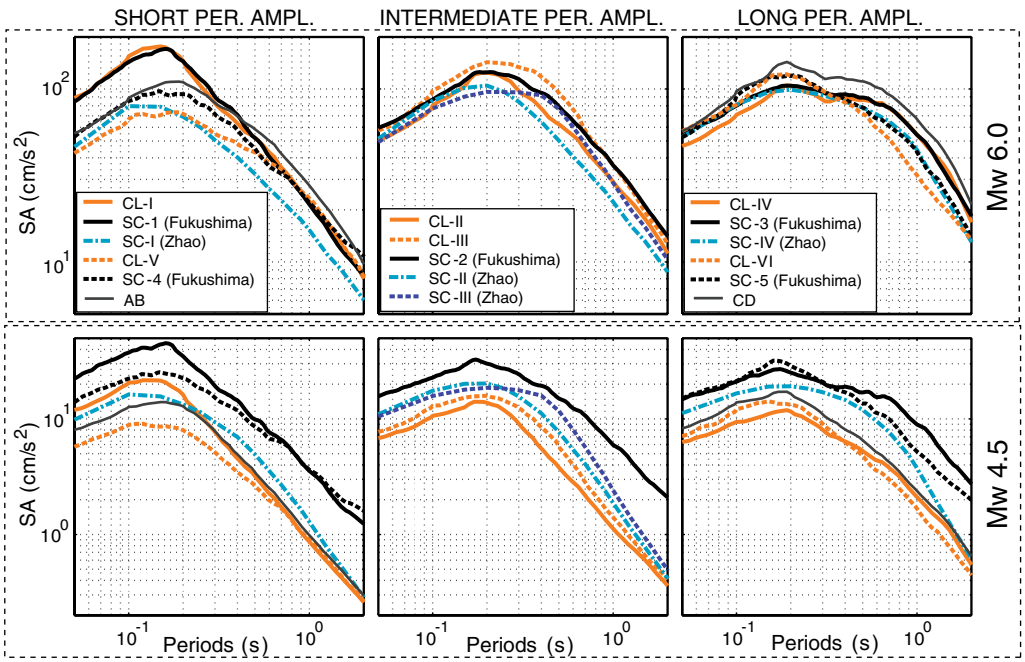

Figure 5. Predicted response spectra for the classification proposed in this study, compared to Zhao *et al.* (2006) and Fukushima *et al.* (2007), whose nomenclature of the site classes is described in Table 2. Spectral ordinates are for moment magnitudes M_w 4.5 and 6.0 (panels from top to the bottom) at hypocentral distance 50 km. Predicted spectra according to Zhao *et al.* (2006) were evaluated for earthquake scenario with focal depths less than 15 km and for unspecified fault type. "PER. AMPL." is the abbreviation for period amplification; site classes that amplify at short periods or have a rock-like behavior are shown in the left panel, site classes that amplify at intermediate periods or have a shallow-soil–like behavior are shown in the central panel, and site classes that amplify at long periods or have a deep-soil–like behavior are shown in the right panel. The color version of this figure is available only in the electronic edition.

of thin soft layers with strong impedance contrast (usually referred to as class E in Eurocode 8 (European Committee for Standardization (CEN), 2004). The high amplitude of class CL-1 as defined in Fukushima *et al.* (2007) was also noticed by those authors; given that their data were mostly from the western Eurasia area, whereas ours are from Italy, the similarity in the results suggests that the high-frequency CL-I amplification could be a global feature. With respect to the original CD site class, the predicted response spectrum for class CL-IV is smaller but maintains a very similar shape. It is typically bimodal, with the longer period lobe that increases in importance as magnitude increases.

In terms of comparisons between GMPEs, Figure 5 indicates that there is satisfactory agreement in the spectral shape of all the GMPEs based on the predominant period in H/V spectral ratios, although there are some differences in amplitudes. The comparison with the Zhao *et al.* (2006) and the Fukushima *et al.* (2007) GMPEs shows fairly good agreement at M_w 6.0, whereas our predicted spectral amplitudes (SA) tend to be somewhat lower at M_w 4.5. We are aware that magnitude uncertainty in small magnitude events may also play a role about the observed discrepancy for M_w 4.5 comparisons. However, all these variations are less than a factor of 2 and do not exceed the usual uncertainty of 0.3 (log base 10). This is an interesting result if we consider the smaller numbers in the Italian dataset, of the order of hundreds of records against thousands of records in Zhao *et al.* (2006). The most noticeable amplitude differences are confined within the classes that amplify at short periods. For instance, at M_w 6.0, the amplitudes of SA for our class CL-I are comparable to those for Fukushima *et al.*'s CL-1 but are larger than Zhao *et al.*'s SA for SC-I; in contrast, the latter is in better agreement with our curves for class CL-V at the same M_w 6.0. The peculiar high amplitude at short periods for class CL-I is also evident when comparing predicted spectra with other non-predominant-period-based GMPEs (these results are shown in the Appendix).

In order to help judge the impact of the new site classification on predicted response spectra, we evaluated whether and to what extent we can achieve a reduction of uncertainty in ground-motion prediction. Overall standard deviation obtained using predominant-period classification and original AB-CD site classes in $\log_{10}$ logarithms are compared in Figure 6a. Figure 6a also shows the inter- and intraevent terms deviation as derived from the regression analysis. Although there is a reduction at short periods when using the period-based site classes, it is small (but comparable to that found by Fukushima *et al.* [2007], as shown in Fig. 6b). Achieving only a small reduction in the variance with the use of more complex site classes is not unexpected and is not a definitive test of the efficacy of a site-classification scheme. In studying a relative small number of motions, Boore (2004) found that the overall variance of individual observations about predicted values decreased only slightly in going from

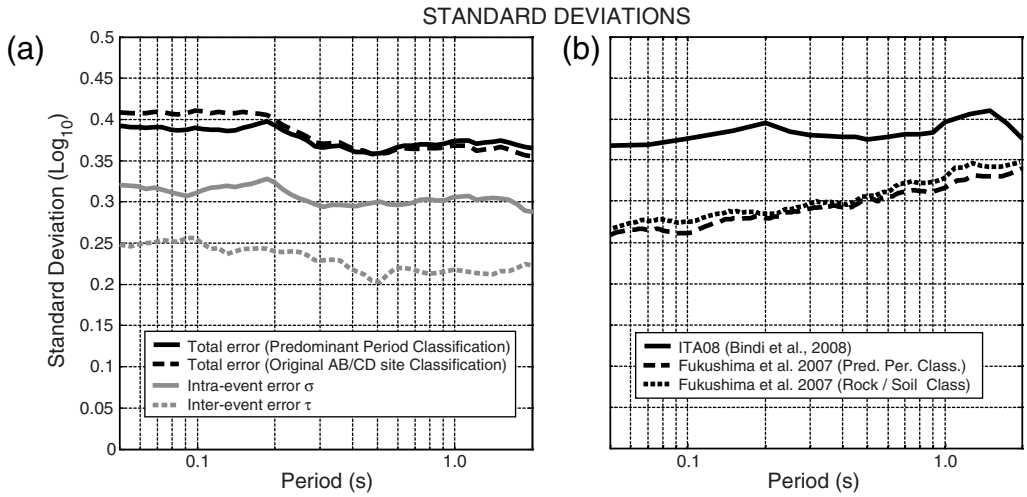

Figure 6. (a) Overall standard deviation obtained using predominant-period classification and original simplified AB and CD site classes in decimal logarithms. Inter and intraevent terms are also shown for the predominant-period classification scheme. (b) Overall standard deviations from Bindi *et al.* (2010) and Fukushima *et al.* (2007) in the same units as stated previously are also provided for comparison. The curve for Fukushima *et al.* (2007) referring to their original rock/soil classification has been kindly provided by the author and allows us to evaluate the reduction in standard deviation those authors achieved when adopting predominant-period classification, analogous to what we show in panel (a).

no classifications to classifications based on continuous V_{S30}, with the largest reduction coming from a rock/soil classification to a National Earthquake Hazard Reduction Program (NEHRP) classification. The more complex schemes, however, did remove systematic trends in the residuals.

In addition, we notice in Figure 6 that the aleatory variation tends to decrease at longer periods, which is in contrast to what Fukushima *et al.* (2007) found with their regression. With either site-classification scheme, our standard deviations are higher than those found in a number of other studies. Others have observed this feature of Italian strong-motion data (e.g., Scasserra *et al.*, 2009; Bindi *et al.*, 2010). Cauzzi and Faccioli (2008) have suggested that the relatively high values of standard deviation at shorter periods could possibly be related to the scatter introduced by site-related amplification effects.

Relative Differences in Amplifications from the GMPEs and from Recordings of the L'Aquila Earthquake

We completed the computation of the coefficients in equation (1) before the occurrence of the 6 April 2009, M_w 6.3 L'Aquila earthquake in central Italy (Chiarabba *et al.*, 2009; Çelebi *et al.*, 2010). It was a normal faulting earthquake that ruptured a 10×25 km^2 fault oriented along the Apennine trend beneath the town of L'Aquila (Cirella *et al.*, 2009; Anzidei *et al.*, 2009; Atzori *et al.*, 2009). Fifty-four accelerometers were triggered, with hypocentral distances from 11 to 277 km. These records gave us the opportunity to investigate how the newly recorded ground motions compare with the predicted values using the predominant-period site classification, including a test on the performance of the site correction terms. Eighteen of the stations that recorded the L'Aquila earthquake had been previously classified in our study; we used the L'Aquila recordings to assign site classes at 36 other stations.

Figure 7 shows the residuals from the L'Aquila earthquake for the different site classes. We grouped the residuals according to their hypocentral distance (within or beyond 100 km, respectively), and we show results in terms of peak

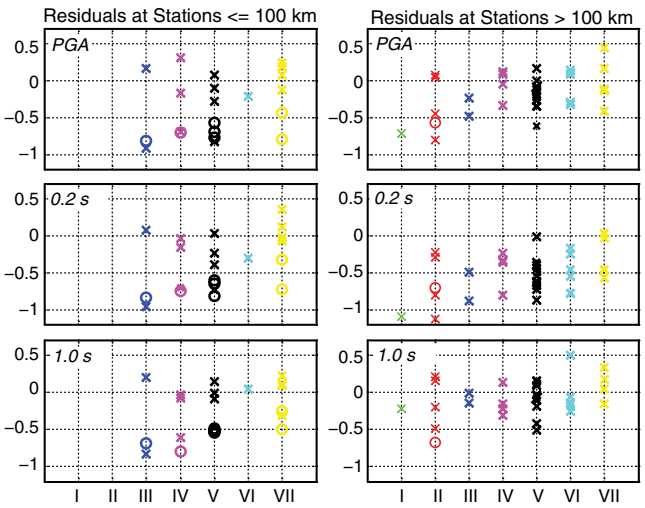

Figure 7. Residuals of PGA and spectral ordinates at 0.2- and 1.0-s periods during the 6 April 2009, M_w 6.3 L'Aquila earthquake. In the panels showing the residuals of predominant-period classes, cross and open circle symbols are used to distinguish stations with source back-azimuth affected by antidirective and directive effects (i.e., whose source-to-station azimuth measured clockwise from north is in the range 57°–187° and 200°–330°, respectively). The color version of this figure is available only in the electronic edition.

ground acceleration (PGA) and spectral ordinates at two selected periods (0.2 and 1.0 s). In Figure 7 crosses and open circle symbols distinguish stations whose source-to-station azimuth measured clockwise from north is in the range of 57°–187° and 200°–330°, respectively. We borrow these ranges from Ameri *et al.* (2009), who, in common with other studies (Pino and Di Luccio, 2009; Bindi, Pacor, *et al.*, 2009; Chioccarelli and Iervolino, 2010), found increasing ground motion southeast of the epicenter and decreasing motion for stations in the opposite direction (this pattern might be due to directivity associated with the propagation of the mainshock rupture). For the purpose of our study, the most important findings from Figure 7 are the similarities in the mean residuals for each class, thus suggesting that the site effect corrections are proper, as they are not producing class-to-class differences in the residuals. The overall negative residuals for this peculiar earthquake are not of concern, and they have been already reported in other papers that studied the event (e.g., Ameri *et al.*, 2009; Akinci *et al.*, 2010; Çelebi *et al.*, 2010).

Finally, the average residuals computed for the L'Aquila earthquake are similar to the interevent residuals at M_w 6.3 from our GMPE regression analysis (see Fig. A1), so we can argue that adding the 6 April 2009 L'Aquila earthquake to the dataset used to compute the regression coefficients would have had little effect on the regression results.

Conclusions and Discussion

In this paper we present a new site-classification scheme for Italian stations, based on the predominant period of the site, as derived from the average horizontal-to-vertical (H/V) spectral ratios of ground motion. This classification scheme is the same as proposed by Zhao *et al.* (2006), with the addition of two classes that account for cases not included in Zhao *et al.* classes. One (which we call CL-V) is defined as a site for which H/V does not exhibit any predominant peaks, with an overall H/V ratio less than 2; the other (CL-VI) also has broad amplifications or multiple peaks in the average H/V ratio at periods larger than 0.2 s. In addition, we include another class (CL-VII) not included in Zhao *et al.* (2006): a catchall class for any site that cannot be placed in the other sites. We then use the new scheme to classify stations in Italy that recorded strong motions, and we then derived GMPEs for these motions (GMPEs were also derived using a simple rock/soil classification scheme).

Despite the relatively small reduction of standard deviation at shorter periods when we use the predominant-period classification, our scheme has the advantage of recognizing well-distinguished behavior of the proposed classes, both in terms of relative amplification with respect to rock site (i.e., AB or CL-V sites) and of predicted spectral shape.

The new CL-V site is useful to classify rock stations to be used as reference sites in site-response studies and in the development of GMPEs. Neither Zhao *et al.* (2006) nor Fukushima *et al.* (2007) included a comparable classification. As a matter of fact, when they were unable to identify a predominant period they used the available geological information to distinguish generic rock or generic soil classes. Figure 4 confirms the validity of our classification criterion: when CL-V is used as reference, the relative amplification tends to unity at short periods for CL-II to CL-VI and at long periods for CL-I.

The predominant-period classification shows interesting results also for class CL-I (predominant period of less than 0.2 s in H/V). The motions for this class have large amplification at short periods relative to CL-V. Zhao *et al.* (2006) assumed that their SC-I is consistent with a stiff class in a geology-based classification. The cross reference between site geologic conditions and predominant-period classification in our study suggests that rock weathering can play a role in high-frequency amplifications observed at rock sites. Also complications in surface topography can amplify ground motions at stiff sites (Pischiutta *et al.*, 2011). Similarly, thin-soft-layer sites (e.g., class E of Eurocode 8 [EC8] from the European Committee for Standardization [CEN], 2004) can also fall in CL-I, contributing to large amplitudes. Weathered rock and class E are quite pervasive and difficult to avoid in practice, and conventional classification criteria are not able to simply recognize them.

Sites with deep-soil profiles (such as CL-IV sites, for instance) are easily recognized in our approach, which also offers the advantage of providing quick and inexpensive site characterization without the necessity of performing time consuming and invasive analysis.

As the predominant-period classification implicitly contains both velocity and thickness of the upper resonant layers in its definition, it may be intrinsically better than using V_{S30} alone. In this sense it is consistent, at least in spirit, with criteria that require the depth of soft upper layers in the site classification, as proposed by Rodríguez-Marek *et al.* (2001), Lang and Schwarz (2006), Pitilakis *et al.* (2006), and Cadet *et al.* (2010).

We also noted that many Italian stations are affected by topographic effects that produce amplification over a broad range of periods (Pischiutta *et al.*, 2011); for this reason there is not a straightforward correlation between site classification based on V_{S30} and our predominant-period-based classification (for example, a number of EC8 sites A are distributed relatively uniformly over all of our classes).

A requirement in the application of our method is that a good mean estimate of the predominant period at a given site is available. Because of the inherent variability in H/V due to such things as angle of incidence and source back-azimuth, a number of recordings at a specific site should be used to obtain stable mean H/V.

Another potential limitation is that we use the predominant period rather than the fundamental period for the whole sediment cover, and therefore the classification based on the proposed method could be controlled by large impedance contrast at shallow depths rather than deeper velocity variations. Class CL-VI deals with this, at least partially, because

it allows for classification of sites for which several significant impedance contrasts in the underlying velocity structure lead to multiple peaks at periods longer than 0.2 s. For engineering applications the higher frequency resonances due to shallow impedance contrasts may be more important than the fundamental mode resonance due to a deeper impedance contrast, and for such sites we prefer to use the predominant period instead of the fundamental period as the basis for the site classification.

We are also aware that our site classifications do not account for sites with very long resonant periods (greater than 2 s). It would be easy to include a class for this case, but Italian sites underlain by deep basins will probably have shallower impedance contrasts, such that there will be predominant periods less than the period of the fundamental mode. Station GBP, installed in the middle of the Gubbio basin over several hundred meters of sediments (Bindi, Parolai, *et al.*, 2009), is a typical example where both the deep alluvium-limestone contrast and an uppermost very soft layer cause both short- (around 0.3 s) and long-period (around 3 s) amplification. According to our classification criteria, station GBP is assigned to a CL-II class if we analyze the range $0 < T < 2$ s; however, it would be classified as CL-VI if we analyze the range $0 < T < 10$ s in a predominant-period criterion (allowing the upper limit of the period-range in the class definition to be 10 s rather than 2 s), whereas looking at the fundamental frequency, station GBP can be classified as a thick sediment site.

Notwithstanding these possible limitations, an encouraging feature of the proposed method relies on the fact that we find a good degree of similarity in our derived GMPEs with those using many more data from other parts of the world, even though deriving GMPEs was not a main goal of this paper.

Finally, we believe that future work should be done to explore the feasibility of using ambient noise to estimate predominant periods from Fourier H/V spectral ratios, thus allowing classification of sites with no earthquake recordings.

Data and Resources

The strong-motion data used in this paper have been recorded by the Rete Accelerometrica Nazionale (RAN). The data, as well as their metadata, are available through the Italian Accelerometric Archive (ITACA) at http://itaca.mi.ingv.it/ItacaNet/ (last accessed June 2011). Both corrected (Massa *et al.*, 2009) and uncorrected waveforms are available for download.

ITACA is the Italian strong-motion database, developed from 2004 in the framework of the 2004–2006 DPC-INGV agreement and includes strong-motion data (1972–2004) from the Italian Accelerometeric Network (RAN), presently operated by the Dipartimento Protezione Civile (DPC), available at http://www.protezionecivile.it (last accessed November 2011); the database includes as well revised earthquakes, recording sites and instrument metadata. An updated and improved release of ITACA has been recently released, including strong-motion data from 2005 to 2007 and records from the latest major earthquakes occurred in Italy (among others, the 2008, M_w 5.4, Parma earthquake and the 2009 L'Aquila seismic sequence).

The supplemental velocity-sensor (Trillium 40-s) seismograms for the selected recent events with $M_w > 4.0$ were recorded by seismological stations of the Italian Seismic Network run by Istituto Nazionale di Geofisica e Vulcanologia (INGV). These waveforms are available at http://iside.rm.ingv.it (last accessed November 2011).

Origin times, epicenter locations, and focal parameters of earthquakes are from the INGV-Centro Nazionale Terremoti website at http://cnt.rm.ingv.it (last accessed August 2011).

More general information on the site classification S4 project adopted for the strong-motion stations can be found at S4 project-Deliverable D8, 2009.

Acknowledgments

This study began as a part of a Cooperative Agreement between the Institute for Radiological Protection and Nuclear Safety (IRSN) and Istituto Nazionale di Geofisica e Volcanologia (INGV) for the years 2005–2007 and continued in Project S4 funded by the Department of Civil Protection of Italy for 2007–2010 (http://esse4.mi.ingv.it). C.D.A. was supported by a fellowship from this project. She spent two years as a visiting scientist at the USGS, Menlo Park, California, and is currently a postdoctoral fellow at PEER Center, University of California, Berkeley, California. We thank the project codirectors, Francesca Pacor and Roberto Paolucci, for their continuous encouragement. The authors acknowledge Antonella Gorini for the assistance in processing the strong-motion data. John Zhao provided the code for the evaluation of his ground-motion prediction equations. Marco Moro provided the GIS-base for the simplified soil classification of the Italian territory, and Giuseppe Di Capua helped with the soil characterization for some stations by means of cooperative information exchange. We also thank Giovanna Calderoni, Fabrizio Cara, Giuseppe Di Giulio, and Giuliano Milana for discussions and useful computational advice. Finally, we thank Dino Bindi, J.B. Fletcher, Sinan Akkar, and John Zhao for useful reviews that improved the paper.

References

Abrahamson, N. A., and W. J. Silva (1997). Empirical response spectral attenuation relations for shallow crustal earthquakes, *Seismol. Res. Lett.* **68,** 94–127.

Akinci, A., L. Malagnini, and F. Sabetta (2010). Characteristics of the strong ground motions from the 6 April 2009 L'Aquila earthquake, Italy, *Soil Dynam. Earthquake Eng.* **30,** 320–335.

Akkar, S., and J. J. Bommer (2006). Influence of long-period filter cut-off on elastic spectral displacements, *Earthquake Eng. Struct. Dynam.* **35,** 1145–1165.

Akkar, S., and J. J. Bommer (2010). Empirical equations for the prediction of PGA, PGV, and spectral accelerations in Europe, the Mediterranean region, and the Middle East, *Seismol. Res. Lett.* **81,** no. 2, 195–206, doi 10.1785/gssrl.81.2.195.

Akkar, S., O. Kale, Y. Yenier, and J. J. Bommer (2011). The high-frequency limit of usable response spectral ordinates from filtered analogue and digital strong-motion accelerograms, *Earthquake Eng. Struct. Dynam.* **40,** doi 10.1002/eqe.1095.

Ameri, G., M. Massa, D. Bindi, E. D'Alema, A. Gorini, L. Luzi, S. Marzorati, F. Pacor, R. Paolucci, R. Puglia, and C. Smerzini (2009). The 6 April 2009, M_w 6.3, L'Aquila (central Italy) earthquake:

Strong-motion observations, *Seismol. Res. Lett.* **36,** 951–966, doi 10.1785/gssrl.80.6.951.

Anzidei, M., E. Boschi, V. Cannelli, R. Devoti, A. Esposito, A. Galvani, D. Melini, G. Pietrantonio, F. Riguzzi, V. Sepe, and E. Serpelloni (2009). Coseismic deformation of the destructive April 6, 2009 L'Aquila earthquake (central Italy) from GPS data, *Geophys. Res. Lett.* **36,** L17307, doi 10.1029/2009GL039145.

Atzori, S., I. Hunstad, M. Chini, S. Salvi, C. Tolomei, C. Bignami, S. Stramondo, E. Trasatti, A. Antonioli, and E. Boschi (2009). Finite fault inversion of DInSAR coseismic displacement of the 2009 L'Aquila earthquake (central Italy), *Geophys. Res. Lett.* **36,** doi 10.1029/2009GL039293.

Beyer, K., and J. J. Bommer (2006). Relationships between median values and between aleatory variabilities for different definitions of the horizontal component of motion, *Bull. Seismol. Soc. Am.* **96,** no. 4A, 1512–1522, doi 10.1785/0120050210.

Bindi, D., L. Luzi, M. Massa, and F. Pacor (2010). Horizontal and vertical ground motion prediction equations derived from the Italian Accelerometric Archive (ITACA), *Bull. Earthquake Eng.* **8,** doi 10.1007/s10518-009-9130-9.

Bindi, D., F. Pacor, L. Luzi, M. Massa, and G. Ameri (2009). The M_w 6.3, 2009 L'Aquila earthquake: Source, path, and site effects from spectral analysis of strong motion data, *Geophys. J. Int.* **179,** doi 10.1111/j.1365-246X.2009.04392.x.

Bindi, D., S. Parolai, F. Cara, G. Di Giulio, G. Ferretti, L. Luzi, G. Monachesi, F. Pacor, and A. Rovelli (2009). Site amplifications observed in the Gubbio basin, central Italy: Hints for lateral propagation effects, *Bull. Seismol. Soc. Am.* **99,** no. 2A, 741–76.

Boore, D. M. (2004). Can site response be predicted?, *J. Earthquake Eng.* **8,** Special Issue 1, 1–4.

Boore, D. M. (2005). On pads and filters: Processing strong-motion data, *Bull. Seismol. Soc. Am.* **95,** 745–750.

Boore, D. M., and M. W. Asten (2008). Comparisons of shear-wave slowness in the Santa Clara Valley, California, using blind interpretations of data from invasive and noninvasive methods, *Bull. Seismol. Soc. Am.* **98,** 1983–2003.

Boore, D. M., and G. M. Atkinson (2008). Ground-motion prediction equations for the average horizontal component of PGA, PGV, and 5%-damped PSA at spectral periods between 0.01 s and 10.0 s, *Earthquake Spectra* **24,** 99–113.

Boore, D. M., and J. J. Bommer (2005). Processing of strong-motion accelerograms: Needs, options and consequences, *Soil Dynam. Earthquake Eng.* **25,** 93–115.

Boore, D. M., C. D. Stephens, and W. B. Joyner (2002). Comment on baseline correction of digital strong-motion data: Examples from the 1999 Hector Mine, California, earthquake, *Bull. Seismol. Soc. Am.* **92,** 1543–1560.

Building Seismic Safety Council (2000). The 2000 NEHRP Recommended Provisions for New Buildings and Other Structures: Part I (Provisions) and Part II (Commentary), FEMA 368/369, Federal Emergency Management Agency, Washington, D.C.

Cadet, H., P. Y. Bard, and A. Rodriguez-Marek (2010). Defining a standard rock site: Propositions based on the KiK-net database, *Bull. Seismol. Soc. Am.* **100,** 172–195.

Cauzzi, C., and E. Faccioli (2008). Broadband (0.05 to 20 s) prediction of displacement response spectra based on worldwide digital records, *J. Seismol.* **12,** doi 10.1007/s10950-008-9098-y.

Çelebi, M., P. Bazzurro, L. Chiaraluce, P. Clemente, L. Decanini, A. DeSortis, W. Ellsworth, A. Gorini, E. Kalkan, S. Marcucci, G. Milana, F. Mollaioli, M. Olivieri, R. Paolucci, D. Rinaldis, A. Rovelli, F. Sabetta, and C. Stephens (2010). Recorded motions of the M_w 6.3 April 6, 2009 L'Aquila (Italy) earthquake and implications for building structural damage: Overview, *Earthquake Spectra* **23,** 651–684, doi 10.1193/1.3450317.

Chiarabba, C., A. Amato, M. Anselmi, P. Baccheschi, I. Bianchi, M. Cattaneo, G. Cecere, L. Chiaraluce, M. G. Ciaccio, P. De Gori, G. De Luca, M. Di Bona, R. Di Stefano, L. Faenza, A. Govoni, L. Improta, F. P. Lucente, A. Marchetti, L. Margheriti, F. Mele, A. Michelini, G. Monachesi, M. Moretti, M. Pastori, M. Piana Agostinetti, D. Piccinini, P. Roselli, D. Seccia, and L. Valoroso (2009). The 2009 L'Aquila (central Italy) M_w 6.3 earthquake: Main shock and aftershocks, *Geophys. Res. Lett.* **36,** L18308, doi 10.1029/2009GL039627.

Chiarabba, C., P. De Gori, L. Chiaraluce, P. Bordoni, M. Cattaneo, M. De Martin, A. Frepoli, A. Michelini, A. Monachesi, M. Moretti, G. P. Augliera, E. D'Alema, M. Frapiccini, A. Gassi, S. Marzorati, P. Di Bartolomeo, S. Gentile, A. Govoni, L. Lovisa, M. Romanelli, G. Ferretti, M. Pasta, D. Spallarossa, and E. Zumino (2005). Mainshocks and aftershocks of the 2002 Molise seismic sequence, southern Italy, *J. Seismol.* **9,** 487–494.

Chioccarelli, E., and I. Iervolino (2010). Near-source seismic demand and pulse-like records: A discussion for L'Aquila earthquake, *Earthquake Eng. Struct. Dynam.* **39,** doi 10.1002/eqe.987.

Cirella, A., A. Piatanesi, M. Cocco, E. Tinti, L. Scognamiglio, A. Michelini, A. Lomax, and E. Boschi (2009). Rupture history of the 2009 L'Aquila earthquake from non-linear joint inversion of strong motion and GPS data, *Geophys. Res. Lett.* **36,** L19304, doi 10.1029/2009GL039795.

Cocco, M., and A. Rovelli (1989). Evidence of the variation of stress drop between normal and thrust faulting earthquakes in Italy, *J. Geophys. Res.* **94,** 9399–9416.

Converse, A. M., and A. G. Brady (1992). BAP-basic strong-motion accelerogram processing software; Version 1.0., *U.S. Geol. Surv. Open-File Rept. 174*, 92–296A.

De Luca, G., S. Marcucci, G. Milana, and T. Sanò (2005). Evidence of low-frequency amplification in the city of L'Aquila, central Italy, through a multidisciplinary approach including strong- and weak-motion data, ambient noise, and numerical modeling, *Bull. Seismol. Soc. Am.* **95,** 1469–1481.

Di Capua, G., G. Lanzo, V. Pessina, S. Peppoloni, and G. Scasserra (2011). The recording stations of the Italian strong motion network: Geological information and site classification, *Bull. Earthquake Eng.* **9,** no. 6, 1779–1796, doi 10.1007/s10518-011-9326-7.

Di Giulio, G., C. Cornou, M. Ohrnberger, M. Wathelet, and A. Rovelli (2006). Deriving wavefield characteristics and shear-velocity profiles from two-dimensional small-aperture arrays analysis of ambient vibrations in a small-size alluvial basin, Colfiorito, Italy, *Bull. Seismol. Soc. Am.* **96,** 1915–1933, doi 10.1785/0120060119.

Douglas, J., and D. M. Boore (2011). High-frequency filtering of strong-motion records, *Bull. Earthquake Eng.* **9,** 395–409, doi 10.1007/s10518-010-9208-4.

Ekström, G., A. Morelli, E. Boschi, and A. M. Dziewonski (1998). Moment tensor analysis of the central Italy earthquake sequence of September–October 1997, *Geophys. Res. Lett.* **25,** 1971–1974.

European Committee for Standardization (CEN) (2004). Eurocode 8: Design of structures for earthquake resistance, part 1: General rules, seismic actions and rules for buildings, EN 1998-1, http://www.cen.eu/cenorm/homepage.htm (last accessed August 2008).

Fukushima, Y., C. Berge-Thierry, P. Volant, D. A. Griot-Pommera, and F. Cotton (2003). Attenuation relation for west Eurasia determined with recent near-fault records from California, Japan and Turkey, *J. Earthquake Eng.* **7,** 1–26.

Fukushima, Y, L. F. Bonilla, O. Scotti, and J. Douglas (2007). Site classification using horizontal-to-vertical response spectral ratios and its impact when deriving empirical ground-motion prediction equations, *J. Earthquake Eng.* **11,** 712–724.

Ghasemi, H., M. Zare, Y. Fukushima, and F. Sinaeian (2009). Applying empirical methods in site classification, using response spectral ratio (H/V): A case study on Iranian strong motion network (ISMN), *Soil Dynam. Earthquake Eng.* **29,** 121–132.

Japan Road Association (1980). *Specifications for Highway Bridges Part V, Seismic Design*, Maruzen Co., LTD, Tokyo, Japan.

Japan Road Association (1990). *Specifications for Highway Bridges Part V, Seismic Design*, Maruzen Co., LTD, Tokyo, Japan.

Joyner, W. B., and D. M. Boore (1993). Methods for regression analysis of strong-motion data, *Bull. Seismol. Soc. Am.* **83,** 469–487.

Lang, D. H., and J. Schwarz (2006). Instrumental subsoil classification of Californian strong-motion sites based on single-station measurements, *Proc. of the 8th U.S. National Conference on Earthquake Engineering* San Francisco, California, United States, 19 April 2006.

Luzi, L., R. Puglia, F. Pacor, M. R. Gallipoli, D. Bindi, and M. Mucciarelli (2011). Proposal for a soil classification based on parameters alternative or complementary to V_{S30}, *Bull. Earthquake Eng.* **9,** doi 10.1007/s10518-011-9274-2.

Luzi, L., S. Hailemikael, D. Bindi, F. Pacor, F. Mele, and F. Sabetta (2008). ITACA (ITalian ACcelerometric Archive): A web portal for the dissemination of Italian strong motion data, *Seismol. Res. Lett.* **79,** no. 5, 716–723. doi 10. 1785/gssrl.79.5

Malagnini, L., A. Rovelli, S. E. Hough, and L. Seeber (1993). Site amplification estimates in the Garigliano Valley, central Italy, based on dense array measurements of ambient noise, *Bull. Seismol. Soc. Am.* **83,** 1744–1755.

Massa, M., F. Pacor, L. Luzi, D. Bindi, G. Milana, F. Sabetta, A. Gorini, and S. Marcucci (2009). The ITalian ACcelerometric Archive (ITACA): Processing of strong-motion data, *Bull. Earthquake Eng.* **8,** doi 10.1007/s10518-009-9152-3

Pacor, F., R. Paolucci, L. Luzi, F. Sabetta, A. Spinelli, A. Gorini, M. Nicoletti, S. Marcucci, L. Filippi, and M. Dolce (2011). Overview of the Italian strong motion database ITACA 1.0, *Bull. Earthquake Eng.* **9,** no. 6, 1723–1739, doi 10.1007/s10518-011-9327-6.

Paolucci, R., A. Rovelli, E. Faccioli, C. Cauzzi, D. Finazzi, M. Vanini, C. Di Alessandro, and G. Calderoni (2008). On the reliability of long period response spectra ordinates from digital accelerograms, *Earthquake Eng. Struct. Dynam.* **37,** 697–710.

Park, D., and Y. M. A. Hashash (2004). Probabilistic seismic hazard analysis with nonlinear site effects in the Mississippi embayment, *Proc. 13th World Conf. Earthq. Eng.* Vancouver, British Columbia, Canada, 1–6 August 2004, CD-Rom Edition, paper no. 1549.

Pino, N. A., and F. Di Luccio (2009). Source complexity of the 6 April 2009 L'Aquila (central Italy) earthquake and its strongest aftershock revealed by elementary seismological analysis, *Geophys. Res. Lett.* **36,** L23305, doi 10.1029/2009GL041331.

Pischiutta, M., A. Rovelli, P. Vannoli, and G. Calderoni (2011). Recurrence of horizontal amplification at rock sites: A test using H/V-based ground motion prediction equations, in *Proc. of 4th IASPEI/IAEE International Symposium "Effects of Surface Geology on Seismic Motion"*, 23–26 August 2011, University of California, Santa Barbara, California.

Pitilakis, K., C. Gazepis, and A. Anastasiadis (2006). Design response spectra and soil classification for seismic code provisions, in G. Bouckovalas (ed) *General Report. Proc. of the Athens Workshop, ETC12, Geotechnical Evaluation and Application of the Seismic Eurocode EC8*, National Technical University of Athens, 20–21 January 2006, Athens, Greece, 31–46.

Pondrelli, S., G. Ekström, and A. Morelli (2001). Seismotectonic re-evaluation of the 1976 Friuli, Italy, seismic sequence, *J. Seismol.* **5,** 73–83.

Rodríguez-Marek, A., J. D. Bray, and N. A. Abrahamson (2001). An empirical geotechnical seismic site response procedure, *Earthquake Spectra* **17,** 65–87.

Rovelli, A., O. Bonamassa, M. Cocco, M. Di Bona, and S. Mazza (1988). Scaling laws and spectral parameters of the ground motion in active extensional areas in Italy, *Bull. Seismol. Soc. Am.* **78,** 530–560.

S4 project-Deliverable D8 (2009). Progress report on Identification of ITACA sites and records with distinctive features in their seismic response, May 2009. Available from http://esse4.mi.ingv.it/ (last accessed November 2011).

Sabetta, F., and A. Pugliese (1996). Estimation of response spectra and simulation of non-stationary earthquake ground motions, *Bull. Seismol. Soc. Am.* **86,** no. 2, 337–35.

Sandıkkaya, M. A., M. T. Yılmaz, B. S. Bakır, and Ö. Yılmaz (2010). Site classification of Turkish national strong-motion stations, *J. Seismol.* **14,** 543–563, doi 10.1007/s10950-009-9182-y.

Scasserra, G., J. P. Stewart, P. Bazzurro, G. Lanzo, and F. Mollaioli (2009). A comparison of NGA ground-motion prediction equations to Italian data, *Bull. Seismol. Soc. Am.* **99,** no. 5, 2961–2978, doi 10.1785/012008013.

Scherbaum, F., J. Schmedes, and F. Cotton (2004). On the conversion of source-to-site distance measures for extended earthquake source models, *Bull. Seismol. Soc. Am.* **94,** 1053–1069.

Spudich, P., W. B. Joyner, A. G. Lindh, D. M. Boore, B. M. Margaris, and J. B. Fletcher (1999). SEA99: A revised ground motion prediction relation for use in extensional tectonic regimes, *Bull. Seismol. Soc. Am.* **89,** 1156–70.

Steidl, J. H. (2000). Site response in Southern California for probabilistic seismic hazard analysis, *Bull. Seismol. Soc. Am.* **90,** 149–169.

Xia, J., R. D. Miller, C. B. Park, J. A. Hunter, J. B. Harris, and J. Ivanov (2002). Comparing shear-wave velocity profiles from multichannel analysis of surface wave with borehole measurements, *Soil Dynam. Earthquake Eng.* **22,** 181–190.

Yamazaki, F., and M. A. Ansary (1997). Horizontal-to-vertical spectrum ratio of earthquake ground motion for site characterization, *Earthquake Eng. Struct. Dynam.* **26,** 671–689.

Zhao, J. X., K. Irikura, J. Zhang, Y. Fukushima, P. G. Somerville, T. Saiki, H. Okada, and T. Takahashi (2004). Site classification for strong-motion stations in Japan using H/V response spectral ratio, in *13th World Conference of Earthquake Engineering* Vancouver, BritishColumbia, Canada, 1–6 August 2004, paper no. 1278.

Zhao, J. X., K. Irikura, J. Zhang, Y. Fukushima, P. G. Somerville, A. Asano, Y. Ohno, T. Oouchi, T. Takahashi, and H. Ogawa (2006). An empirical site-classification method for strong-motion stations in Japan using H/V response spectral ratio, *Bull. Seismol. Soc. Am.* **96,** 914–925.

Appendix

Regression Analysis, Residuals, and Comparison between GMPEs

Method

The regression analysis is performed using the one-step method of Joyner and Boore (1993). This method provides both inter- and intraevent residuals and estimate of the corresponding standard deviations. Equation (1) is linearized through a Taylor series and solved iteratively. Fukushima *et al.* (2003, 2007) found that $f(T)$ was equal to 0.42 using European earthquakes. We used the same value in order to simplify the linearization problem. (Ⓔ The values found for the coefficients of equation 1 are listed in Table S1, available in the electronic supplement to this paper.)

Residuals

Residuals of the predictive equations are computed as the logarithmic ratio between observed and predicted response spectra. We plotted the interevent residuals (e.g., Bindi, Pacor, *et al.*, 2009; Scasserra *et al.*, 2009) for PGA with respect to moment magnitude (Fig. A1). We also show an example of intraevent residuals for PGA with respect to moment magnitude (Fig. A2) and hypocentral distance (Fig. A3), distinguishing the different predominant-period classes. Misfits do not seem to be biased either in magnitude

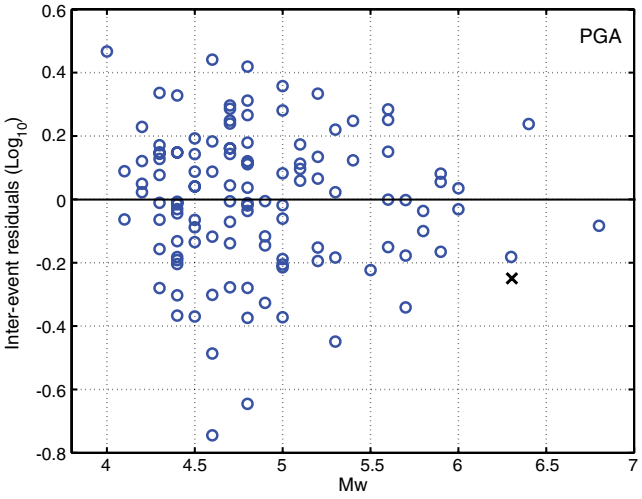

Figure A1 Dependence of interevent PGA residuals on moment magnitude M_w. The cross symbol shows the average residual computed for all the April 6, 2009 L'Aquila earthquake records in a predominant-period site-classification scheme. The color version of this figure is available only in the electronic edition.

or in distance, as they oscillate around zero and do not show any significant trends. (Ⓔ Residuals for 0.2 s and 1.0 s are available in the electronic supplement to this paper in Fig. S3, S4, S5, and S6.)

Comparison with Other Regressions

Figure A4 shows the effect of our site-classification on predicted response spectra, compared to the trend shown by another predictive equation recently published by Bindi *et al.* (2010) for the Italian data using substantially the same dataset (Fig. A5 is similar to Figure 5, but the latter includes a comparison with GMPEs that used predominant-period-based site classes and data from other parts of the world). The GMPEs by Bindi *et al.* (2010) (hereby referred to as ITA08) use three site classes (rock, shallow, and deep-soil). While ITA08-predicted spectra for rock sites agree fairly well with our predictions for CL-V sites, ITA08 predictions for shallow soils agree with our CL-II and CL-III spectra at short periods but they are smaller than our predictions at longer periods.

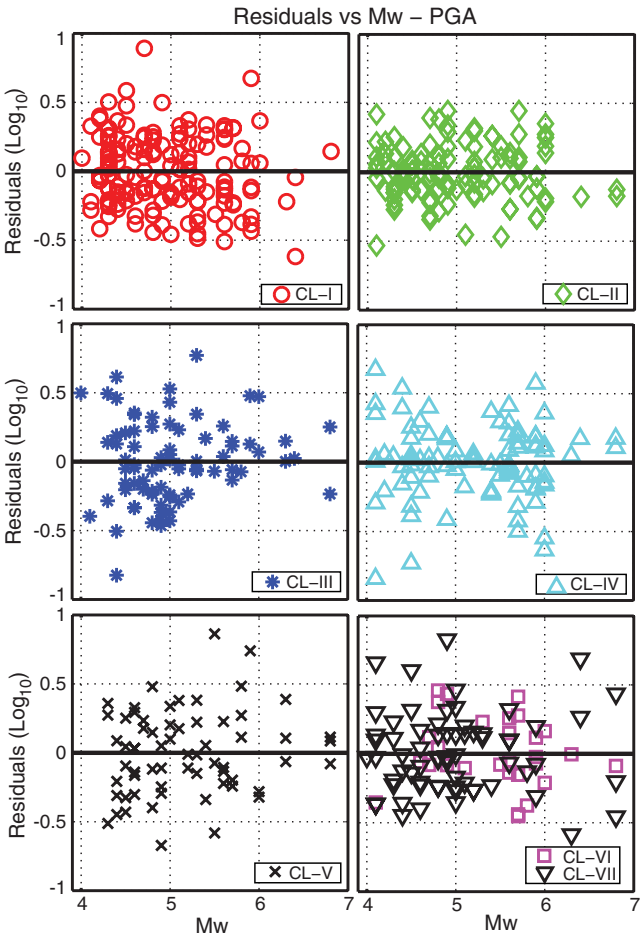

Figure A2 Dependence of intraevent residuals on moment magnitude M_w at PGA for the different predominant-period classes proposed in this study. The color version of this figure is available only in the electronic edition.

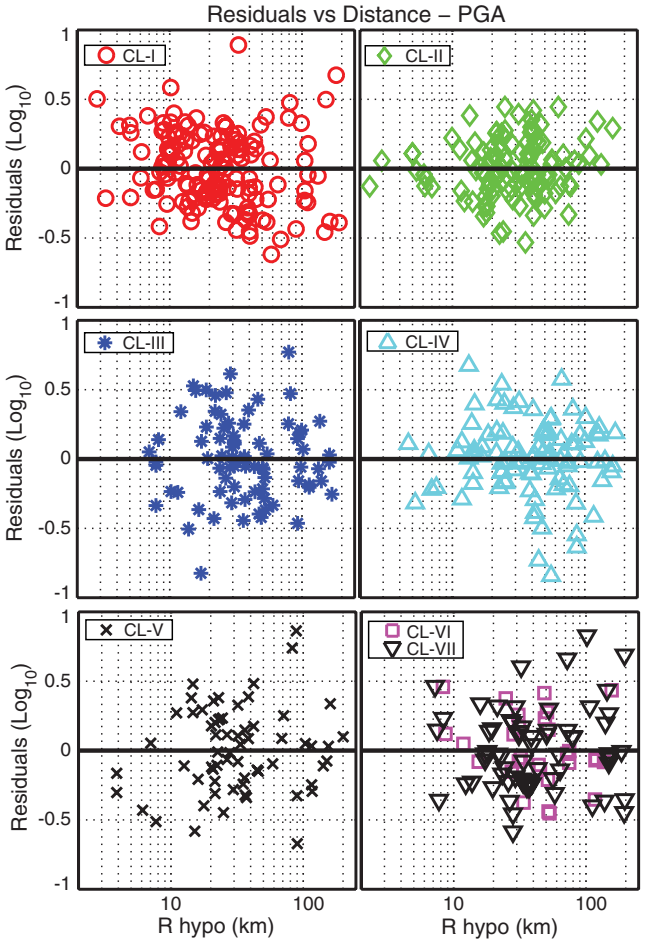

Figure A3 Dependence of intraevent residuals on hypocentral distance Rhypo at PGA for the different predominant-period classes proposed in this study. The color version of this figure is available only in the electronic edition.

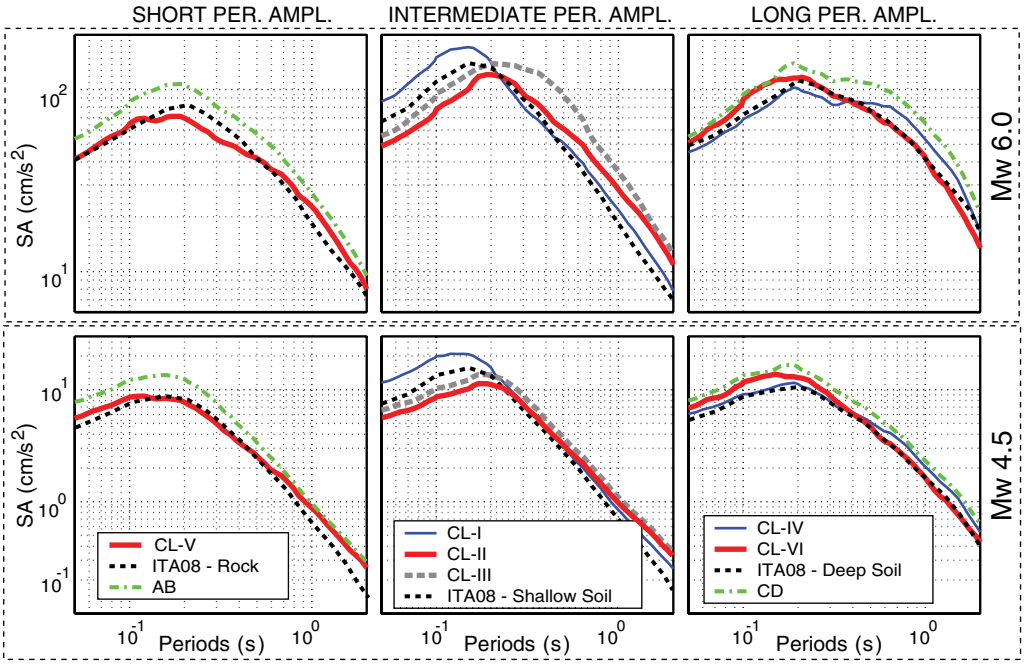

Figure A4 Predicted response spectra for the classification proposed in this study, compared to Bindi *et al.* (2010), referred to as ITA08. Spectral ordinates are for moment magnitudes M_w 4.5 and 6.0 (panels from top to the bottom) at hypocentral distance compatible to 50 km of hypocentral distance. "PER. AMPL." is the abbreviation for "period amplification"; site classes that amplify at short periods or have a rock-like behavior are shown in the left panel, site classes that amplify at intermediate periods or have a shallow-soil–like behavior are shown in the central panel and site classes that amplify at long periods or have a deep-soil–like behavior are shown in the right panel. The color version of this figure is available only in the electronic edition.

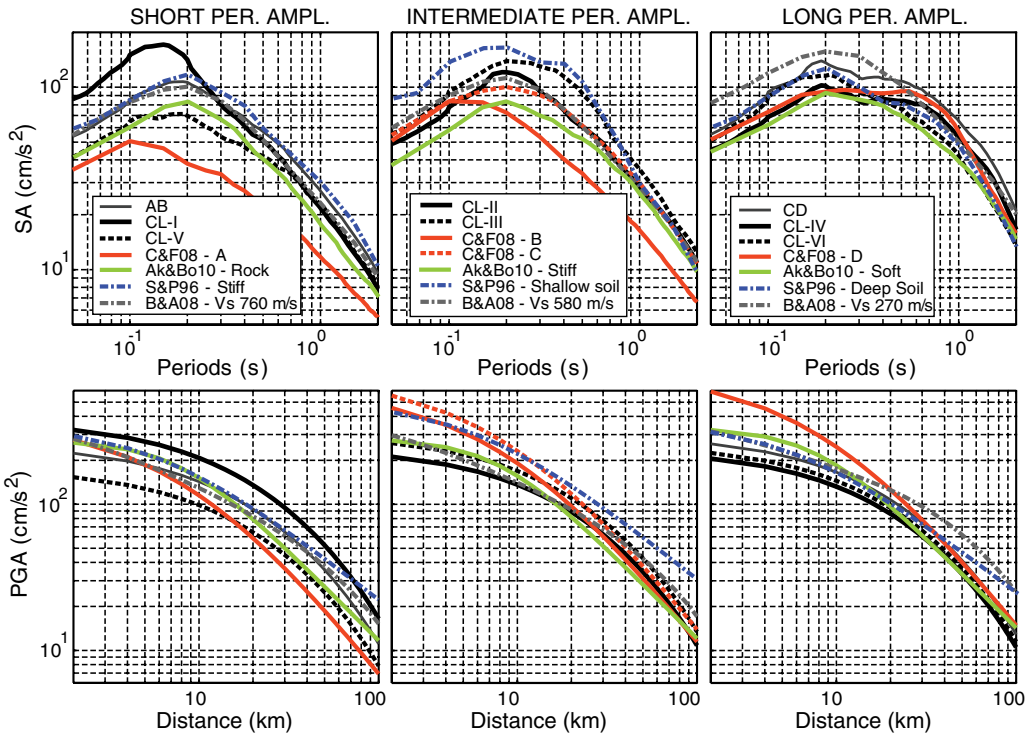

Figure A5. (Top panels) Comparison between our predicted spectral amplitudes and those from other global or regional predictions based on non-site-period classification criteria for moment magnitudes M_w 6.0 at distances compatible to 50 km of hypocentral distance. (Bottom panels) PGA with respect to Joyner and Boore distance (Rjb) for the same GMPEs considered in the top panels. Consistency in the distance metric is obtained by using the distance conversion scheme proposed by Scherbaum *et al.* (2004). Refer to Figure A4 for the criterion used to arrange the plots. The color version of this figure is available only in the electronic edition.

Furthermore, ITA08 spectra for shallow soils are peaked at somewhat shorter periods than our CL-II and CL-III: the peaked period is more consistent with our CL-I predictions, but ITA08 spectra show 33% lower amplitudes. Finally, ITA08 predictions for deep soils agree with our CL-IV spectra up to 0.5 s at M_w 4.5 and 6.0. Notwithstanding the databases used to derive the predictive equations are fairly similar, the differences in spectral values can be essentially due to the fact that the classification scheme used is very different, ITA08's one being based on schematic geologic classification. Irregularities in surface topography and layering, velocity inversions, deep refractors and scatterers, superficial weathering, and other causes may be responsible for the differences between our approach and ITA08.

Figure A5 shows the comparison between our predicted spectra and other global or regional predictions for which site classes are not based on the predominant period: it does address epistemic uncertainty related to the variability of mean predictions for a particular site. The comparison is performed among the GMPEs based on European seismic code classes (Cauzzi and Faccioli, 2008, hereby referred to as C&F08), V_{S30} classes (Boore and Atkinson, 2008, hereby referred to as B&A08) and generic soil description (Akkar and Bommer, 2010, and Sabetta and Pugliese, 1996, hereby referred to as Ak&Bo10 and S&P96, respectively). In order to ensure consistency among the horizontal component definition for the different GMPEs included in our comparison, the predicted spectral amplitudes of S&P96 and ITA08 (which are estimated for the largest horizontal component) have been corrected according to the simple linear relationship proposed by Beyer and Bommer (2006). We did not correct the predicted spectral amplitudes of B&A08 because, as mentioned in Beyer and Bommer (2006), the average difference between GMRotI50 and the geometric mean of the two horizontal components is negligible.

In the panels, predicted spectra are computed for the same moment magnitude 6.0, where all the GMPEs are well constrained. Using a similar criterion to the one of Figure A4, panels have been arranged in order to separate sites that amplify short periods or have a rock-like behavior (left panels) from sites that amplify long periods or have deep sedimentary layers (right panels). The graphs in the central panel show motions for sites that amplify intermediate periods or have shallow soil layers. In order to ensure compatibility between different distance metrics, we exploited the distance conversion approach proposed by Scherbaum *et al.* (2004) based on statistical analysis of matching distance types up to 100 km in terms of Joyner and Boore distance (hereby referred to as Rjb) for three possible faulting styles. We selected the option for generic fault type (dip angles between 40° and 90°) and computed compatible hypocentral and epicentral distances for each of the selected magnitudes of Figure A4, starting from a linear array of Rjb. In Figure A5, spectral amplitudes are evaluated at distances compatible to a 50-km hypocentral distance. The same figure shows the distance scaling of the PGA with respect to Rjb.

The comparison among different GMPEs included in the plot shows a big variability among the different authors. In general, however, the difference between our GMPEs and other authors' does not exceed a factor of 2. The unique exception is class CL-I, which shows significantly larger spectral ordinates at short periods. As discussed in the text (Fig. 6), we have differentiated spectra of CL-I from the other predicted spectra for rock/stiff site conditions. This result confirms the necessity to distinguish sites that amplify at short periods from sites that show limited or no amplification (CL-V).

Despite some minor differences among the various GMPEs mainly due to different short and long distance attenuation terms in their functional forms, we can note that at low magnitudes, S&P96 shows the biggest differences with respect to our predictions. However, we wanted to include their predictions in the comparisons because their predictive equations have been used frequently in Italy. (Ⓔ Plots showing the distance scaling for 0.1 s, 0.3 s, and 1.0 s are available in the electronic supplement to this paper in Fig. S7.)

Istituto Nazionale di Geofisica e Volcanologia (INGV)
Via di Vigna Murata, 605
00143 Roma, Italy
carola.dialessandro@berkeley.edu
antonio.rovelli@ingv.it
(C.D.A., A.R.)

Institut Français des Sciences et Technologies
des Transports de l'Aménagement et des Réseaux (IFSTTAR)
Département Géotechnique, Eau et Risques
Groupe Séismes et Vibrations
58 boulevard Lefebvre
75732 Paris Cedex 15, France
fabian.bonilla@lcpc.fr
(L.F.B.)

U.S. Geological Survey
MS 977 345 Middlefield Road
Menlo Park, California 94025
boore@usgs.gov
(D.M.B.)

Institute for Radiological Protection and Nuclear Safety (IRSN)
31, avenue de la Division Leclerc
92260 Fontenay-aux-Roses, France
oona.scotti@irsn.fr
(O.S.)

Manuscript received 22 March 2011